Processing and Application of Ceramics 12 [4] (2018) 313–318
https://doi.org/10.2298/PAC1804313L

BY-NC-ND

Improved mechanical properties of dense β-Si_3N_4 ceramics fabricated by spark plasma sintering with Al_2O_3-YSZ additives

Yang Li[1], Weiqin Ao[2,*], Jihua Gao[1], Chaohua Zhang[1], Fusheng Liu[1], Yong Du[2,*]

[1]*College of Materials Science and Engineering, Shenzhen University and Shenzhen Key Laboratory of Special Functional Materials, Shenzhen 518060, PR China*
[2]*State Key Laboratory of Powder Metallurgy, Central South University, Changsha, Hunan 410083, PR China*

Received 24 May 2018; Received in revised form 31 August 2018; Accepted 25 October 2018

Abstract

In this work the influence of sintering conditions on structure and mechanical properties of Si3N4 ceramics was investigated. Nearly full dense β-Si_3N_4 ceramics with excellent mechanical properties and interlock microstructure of elongated grains was fabricated using Al_2O_3 and yttria-stabilized zirconia (YSZ with 3 mol% Y_2O_3) as sintering additives by spark plasma sintering (SPS) at relatively low temperature of 1600 °C for 15 min. X-ray diffraction analysis shows that the SPSed sample is pure β-Si_3N_4 phase without any secondary crystalline phase. The elements Al, Zr, Y and O of the additive can diffuse into Si_3N_4 lattice forming β-Si_3N_4-based solid solution. The residual additive formed an amorphous phase at the β-Si_3N_4 grain boundaries. The β-Si_3N_4 ceramics obtained by SPS using 6.0 wt.% Al_2O_3 and 6.0 wt.% YSZ as additives shows interlock elongated β-Si_3N_4 grains of 500 nm in width and 3000 nm in length, high density of 3.29 g/cm^3, Vickers hardness of 16.15 GPa and high fracture toughness K_{IC} of 6.75 MPa m$^{1/2}$.

Keywords: *Si_3N_4, spark plasma sintering, sintering additives, mechanical properties, microstructure*

I. Introduction

Advanced ceramics and their composites have been developed for a number of commercial and industrial applications, such as turbine engines, electronic packaging and cutting tools [1–5]. Silicon nitride is one of the most promising advanced ceramics materials due to its low density, high temperature strength, excellent thermal shock resistance, which can be widely used in cutting tools, bearings, reciprocating engine parts, wear and metal forming components and springs [6–8]. Two phase structures exist in Si_3N_4 ceramics, the low temperature structure α-Si_3N_4 and the high temperature structure β-Si_3N_4 [9]. The large, elongated β-Si_3N_4 grains with high aspect ratio deflect the propagation of cracks, and thus increase the fracture toughness of the material [10]. Therefore, manufacturing of the dense β-Si_3N_4 with interlocking microstructures of elongated grains plays an important role in the high mechanical properties of silicon nitride ceramics for many structural applications [11].

Si_3N_4 is difficult to densify by solid state sintering because of its high degree of covalent bonding, thus liquid-phase sintering with suitable additives is a preferred method of promoting densification. Various metal oxides such as lanthanide oxides and rare earth oxides were used as sintering additives. Conventional sintering techniques, such as pressureless sintering [12], reaction bonding sintering [13], gas pressure sintering [14], hot pressing sintering [15] and hot isostatic pressing sintering etc. [16], usually need high sintering temperature, slow heating rate and long holding time to obtain fully dense materials and fabricate silicon nitride ceramics with sintering additives. Spark plasma sintering (SPS) is known for its high efficiency to densify ceramics at relatively low temperature under compression, using pulsed DC current through punches and graphite die. The pulsed DC current promotes a fast heating of the powder by charging the intervals between powder particles with electrical energy and effectively applying a high-temperature spark plasma. It is one of the most innovative and promising methods for producing silicon nitride [17]. It has been reported that SPS has

*Corresponding authors: tel: +86 0755 26535133,
e-mail: *aomily@126.com*

been used to fabricate highly dense β-Si_3N_4, at 1600 °C for 5 min [18], at 1500 °C for 5 min [19] or at 1700 °C for 5 min [20], using Y_2O_3 and Al_2O_3 as sintering additives, or at 1700 °C for 5 min using $BaCO_3$, SiO_2 and Al_2O_3 as sintering additives [21]. The composites in ZrO_2-Al_2O_3 system have the potential to combine an increased hardness with excellent toughness of tetragonal zirconia. The equimolecular mixtures of α- and β-Si_3N_4 with high density, Vickers hardness of 6–12 GPa and fracture toughness of 3.7–6.2 MPa $m^{1/2}$ were fabricated by hot-pressing using ZrO_2 and Al_2O_3 as sintering additives [22].

In this work, a nearly full dense β-Si_3N_4 ceramics with interlock microstructure of elongated grains, showing good Vickers hardness of 16.15 GPa and fracture toughness K_{IC} of 6.75 MPa $m^{1/2}$, was fabricated using Al_2O_3 and yttria-stabilized zirconia (YSZ with 3 mol% Y_2O_3) as sintering additives by spark plasma sintering (SPS) at relative low temperature of 1600 °C for 15 min.

II. Experimental procedure

Si_3N_4 (95% α-phase, SN-E10 grade, 0.6 μm, UBE Industries, Japan), Al_2O_3 (Meryer, 100 nm, Germany) and YSZ (3 mol% Y_2O_3, 100 nm, King's Ceramics & Chemicals Co., LTD) powders were used as starting materials in this study. These powders were mixed according to the weight radios of Si_3N_4 : Al_2O_3 : YSZ = 88 : 6 : 6 by wet ball-milling in ethanol for 8 h using zirconia balls and high density polyethylene jar. The weight ratio of balls to powders was kept at about 10 : 1. The zirconia balls with 3.5 and 5.0 mm in diameter and their weight ratio of 8 : 2 were used. The milled powders were dried and sintered by SPS (lab-made SPS system) in vacuum lower than 1.0×10^{-2} Pa using a high strength cylindrical graphite die with the inner diameter of 30 mm. The heating process was controlled by an optical pyrometer (Raytek) focused on the surface of the die. The samples were heated to the final sintering temperature, 1450 or 1600 °C, at heating rate of 100 °C/min, held at this temperature for 15 min and then cooled down to room temperature at rate of 100 °C/min. The initial pressure of 15.0 MPa was applied before heating and further pressure of 45 MPa was applied above 1000 °C.

The sintered samples were polished using <1 μm diamond paste. The density of the sintered sample was measured by the Archimedes method. The phases of the samples were analysed by X-ray diffraction (XRD) using a Bruker D8 Advance SS/18 kW diffractometer with CuKα radiation and Jade 6.5 software and the microstructures were observed by scanning electron microscopy (SEM) with energy dispersive X-ray spectroscopy (EDS) (Su-70, Hitachi). The Rietveld refinements of XRD patterns, performed by Topas 3.1 software, were used to estimate the theoretical density of the sample. Hardness and fracture toughness were determined using indentation technique. The hardness of the polished surface of the bulk sample was measured on a hardness tester (Micro-586 Vickers Hardness Tester, Shanghai Tianiin Optical Instrument Co., Ltd.) with an indentation load of 98 N and a dwell time of 15 s. The fracture toughness K_{IC} was determined from the measurement of the crack length based on the equation [23]:

$$K_{IC} = 0.016\left(\frac{E}{H}\right)^{1/2}\frac{1000P}{C^{3/2}} \quad (1)$$

where K_{IC} is fracture toughness, E is Young's modulus (300 GPa for Si_3N_4 in this work [23]), H is the Vickers hardness, P is the indentation load and C is the mean crack length measured from the centre of the indentation.

III. Results and discussion

3.1. Densities

A high density of the Si_3N_4 ceramics was obtained by SPS using 6.0 wt.% Al_2O_3 and 6.0 wt.% YSZ as additives at relatively low temperature, which is important for many structure applications. The density was 3.255 g/cm^3 for the sample SPSed at 1450 °C for 15 min and 3.290 g/cm^3 for the sample SPSed at 1600 °C for 15 min, under the pressure of 45 MPa. This is nearly full density of the Si_3N_4-6.0 Al_2O_3-6.0 YSZ composite as compared to its theoretical density of 3.36 g/cm^3, estimated by Rietveld refinement from its XRD pattern and EDS results. The small amount of Al, Zr and Y was considered to occupy the Si site of β-Si_3N_4 lattice, while O occupies the N site of β-Si_3N_4 lattice. The small amount of the glass phase at the grain boundary of β-Si_3N_4 phase was ignored in this calculation. This density is higher than reported in relative literature. Thus, it is reported that the density of 3.25 g/cm^3 of Si_3N_4 ceramics was obtained by SPS using 9.0 wt.% Al_2O_3 and 6.0 wt.% Y_2O_3 additives at 1650 °C for 10 min [24]. The silicon nitride ceramics obtained by SPS with a density of 3.08 g/cm^3 sintered at 1500 °C, 3.23 g/cm^3 sintered at 1600 °C and also 3.23 g/cm^3 sintered at 1650 °C, by using 2.0 wt.% Al_2O_3 and 5.0 wt.% Y_2O_3 additive was also reported [25]. Hayashi *et al.* [26] reported that the ceramic material obtained by sintering in a graphite resistance furnace at 1900 °C for 2 to 48 h under a nitrogen pressure of 0.9 MPa had a density ranging from 3.20 to 3.26 g/cm^3 with $MgSiN_2$ as an additive. Ewais *et al.* [22] reported that the silicon nitride ceramics obtained by hot pressing sintering at 1800 °C for 20 min under pressure of 30 MPa in CO/CO_2 atmosphere had a density of 2.93 g/cm^3 by using 5.0 wt.% ZrO_2 and 5.0 wt.% Al_2O_3 as additives and 3.26 g/cm^3 by using 10.0 wt.% ZrO_2 and 10 wt.% Al_2O_3 additive.

3.2. Phase and microstructure

Figure 1 shows the XRD patterns for the raw Si_3N_4 powders, mixed powders with 6.0 wt.% Al_2O_3 and 6.0 wt.% YSZ additives and the samples sintered at 1450 °C and 1600 °C. It is obvious that the raw powder contains α-Si_3N_4 main phase with minor β-Si_3N_4 phase, shown in Fig. 1a. The Al_2O_3 and YSZ additive phases,

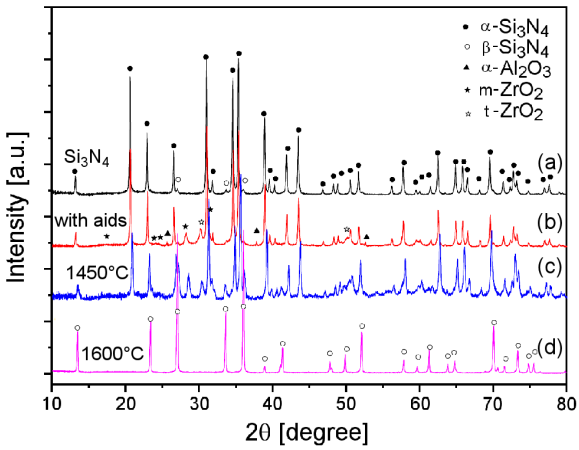

Figure 1. XRD patterns for: a) the raw Si_3N_4 powders, b) mixed powders with 6.0 wt.% Al_2O_3 and 6.0 wt.% YSZ additives, c) the samples sintered at 1450 °C and d) 1600 °C for 15 min

α-Al_2O_3, monoclinic (m) ZrO_2 and tetragonal (t) ZrO_2, appear in the mixed powder, shown in Fig. 1b. As the mixed powder was sintered at 1450 °C for 15 min, the amount of β-Si_3N_4 phase increases, but α-Si_3N_4, α-Al_2O_3, m-ZrO_2 and t-ZrO_2 phases are kept, shown in Fig. 1c. However, the pure β-Si_3N_4 phase was obtained without any other crystalline phases in the sample sintered at 1600 °C for 15 min, shown in Fig. 1d.

Figure 2 shows the SEM images for the fracture surfaces of the samples SPSed at 1450 °C and 1600 °C for 15 min. Combining XRD analysis, it is found the typical α-Si_3N_4 equiaxed hexagonal grains of about 600 nm formed in the sample SPSed at 1450 °C, together with the additive phases at the α-Si_3N_4 grain boundaries, shown in Fig. 2a. By contrast, the uniform interlock microstructure of the elongated β-Si_3N_4, with 500 nm in width and 3000 nm in length, is developed in the sample SPSed at 1600 °C without any secondary crystalline phase, shown in Fig. 2b.

A typical back scattering electron micrograph of the polished surface of the sample SPSed at 1600 °C is shown in Fig. 3a. It indicates that fully dense and uniform interlock microstructure of the elongated β-Si_3N_4 was obtained in this sample. It consists of two phase regions, the elongated dark region and the white region. Based on the results from XRD analysis and the compositions obtained by the quantitative EDS analysis, we confirmed that the dark region belongs to the β-Si_3N_4 phase. The white region is the glass phase formed from the residual additives at the boundaries of the β-Si_3N_4 grains. The typical EDS results for the dark and white regions are shown in Figs. 3b and 3c. The EDS results from larger elongated β-Si_3N_4 dark region may be more precise, which contains the elements Al, Zr, Y and O (Fig. 3b). It is reasonable to believe that these elements from the additives can diffuse into β-Si_3N_4 phase, forming β-Si_3N_4 solid solution. The large amount of Si and N appeared in the glass phase at the grain boundary. However, EDS is probably affected by β-Si_3N_4 matrix due to the very thin glass layer (about 80 nm).

The phase transformation behaviour during the densification can be explained by considering the distinct types of grain boundary phase [11]. The Al_2O_3 and YSZ additive phases, α-Al_2O_3, m-ZrO_2 and t-ZrO_2 around Si_3N_4 phase were kept as the mixed powder sintered at 1450 °C. However, they form the liquid glass phase at the grain boundary of Si_3N_4 according to the ZrO_2-Al_2O_3-SiO_2 phase diagram [27] as the mixed powder was sintered at 1600 °C by the reaction with the SiO_2 (2 wt.%) covering the Si_3N_4 particles. Silica layer may exist in the starting Si_3N_4 powders provided by the supplier. Sintering at this temperature causes grains growth of elongated β-Si_3N_4 resulting from the diffusion-dominated solution-precipitation process. The melted glass has enough fluidity to dissolve the α-Si_3N_4 grains, but β-Si_3N_4 grains precipitated from the melt at this temperature. Super saturation provides the driving force for fast nucleation of β-Si_3N_4 crystallites. Coalescence of precipitated β-Si_3N_4 crystallites speeds up the growth of elongated β-Si_3N_4 grains instead of the slower atomic diffusion since it is energetically favourable as it indirectly reduces the supersaturation of dissolved Si_3N_4.

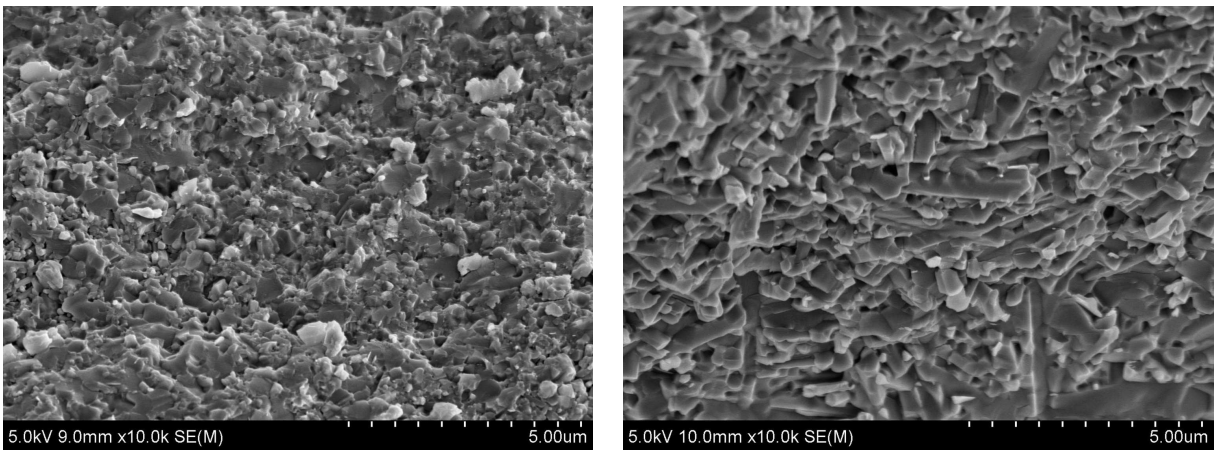

(a) (b)

Figure 2. SEM images of the fracture surfaces for the samples SPSed at: a) 1450 °C and b) 1600 °C for 15 min

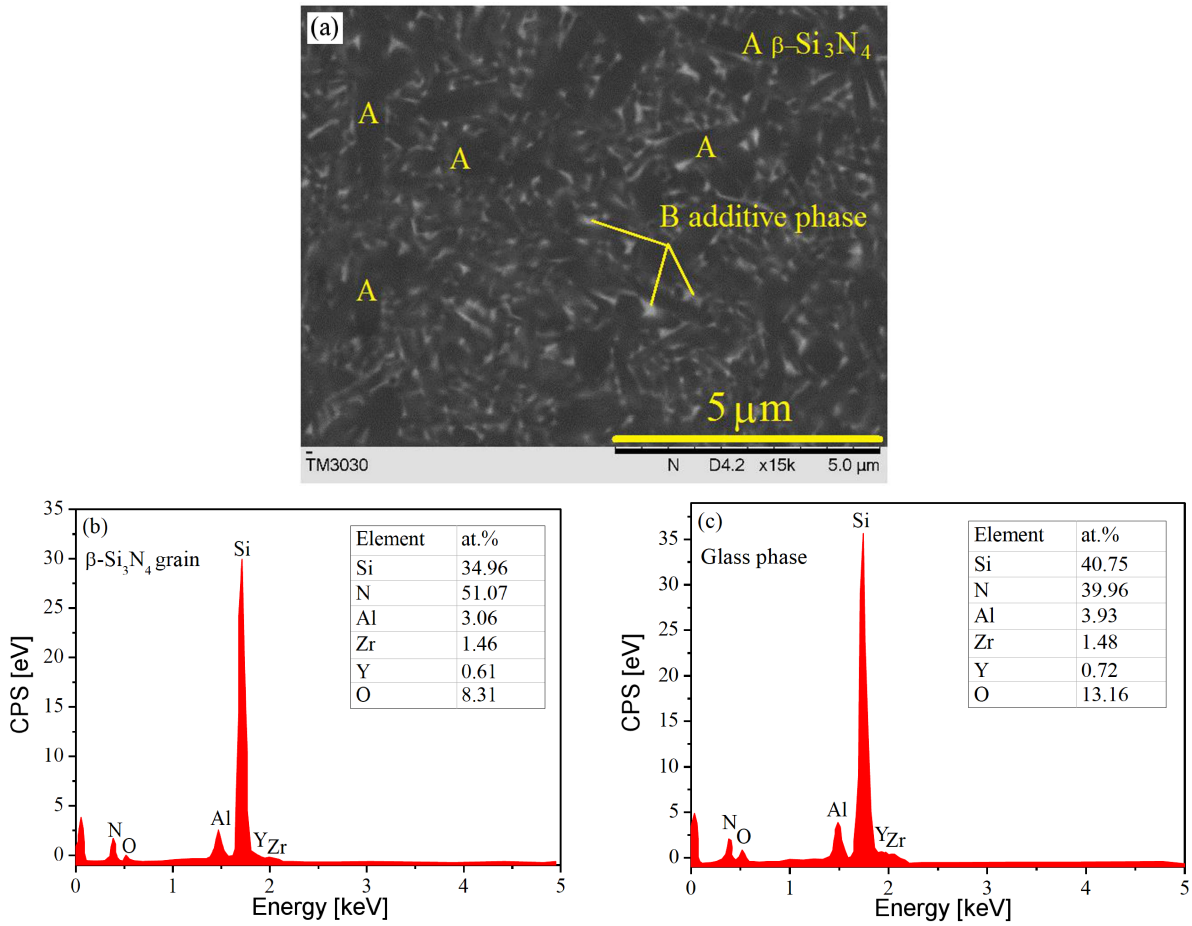

Figure 3. Typical backscattered electron micrograph (a), the EDS images and analysis results for the elongated dark region (β-Si_3N_4 phase) (b) and the white region (glass phase) (c) in the micrograph of the polished surface of the sample SPSed at 1600 °C for 15 min

Table 1. The relative content of Al_2O_3 and MgO at different points shown in Fig. 7

Sample	ρ [g/cm^3]	H_v [GPa]	K_{IC} [MPa m$^{1/2}$]	Phase
Si_3N_4 at 1450 °C	3.255	18.15	3.39	α-Si_3N_4 + β-Si_3N_4 + α-Al_2O_3 + m-ZrO_2 + t-ZrO_2
Si_3N_4 at 1650 °C	3.289	16.13	6.75	β-Si_3N_4 + Glass

3.3. *Hardness and fracture toughness*

Hardness and fracture toughness were determined using indentation technique. Figure 4 shows a typical Vickers fingerprint on the sample SPSed at 1600 °C for 15 min. The Vickers hardness and fracture toughness of the obtained silicon nitride ceramics in this work are 18.15 GPa and 3.39 MPa m$^{1/2}$ for the ceramics SPSed at 1450 °C, and 16.13 GPa and 6.75 MPa m$^{1/2}$ for the ceramics SPSed at 1600 °C, respectively (Table 1). The higher Vickers hardness but lower fracture toughness in the sample SPSed at 1450 °C is due to its α-Si_3N_4 main phase with weak bonding strength to crystalline Al_2O_3 and YSZ additives. On the other hand, the slightly lower Vickers hardness but much higher fracture toughness in the sample SPSed at 1600 °C is due to the sample's pure β-Si_3N_4 phase having strong bonding strength with the glass formed by Al_2O_3 and YSZ additives. It is known that the hardness of α-Si_3N_4 is higher than that of β-Si_3N_4 [24], while β-Si_3N_4 phase shows better fracture toughness [10]. The sample SPSed at 1600 °C for 15 min using Al_2O_3 and yttria-stabilized zirconia additives shows relatively good mechanical properties with Vickers hardness of 16.13 GPa and fracture toughness

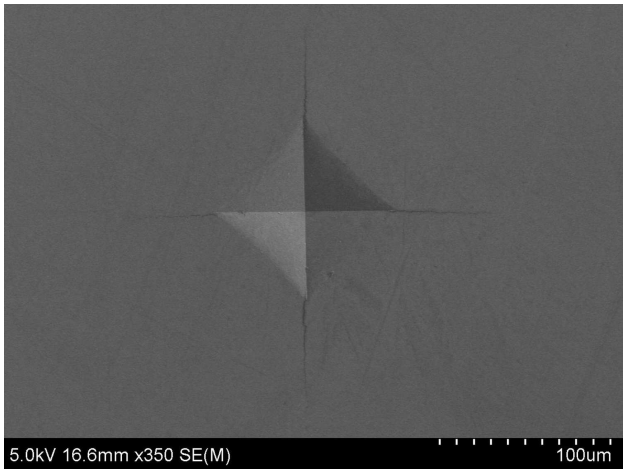

Figure 4. Vickers indent on of the SPSed Si_3N_4 at 1600 °C for 15 min with 6.0 wt.% Al_2O_3 and 6.0 wt.% YSZ

of 6.75 MPa $m^{1/2}$ as compared to other literature reports. It is reported that the Vickers hardness of 11 GPa and toughness of 5.6 MPa $m^{1/2}$ were obtained for Si_3N_4 by SPS using $BaCO_3$, SiO_2 and Al_2O_3 sintering additives [21]. The Vickers hardness of 6–12 GPa and fracture toughness of 3.7–6.2 MPa $m^{1/2}$ were obtained for Si_3N_4 by hot-pressing using ZrO_2 and Al_2O_3 as sintering additives [22]. The Vickers hardness of 14.92 GPa and fracture toughness of 6.44 MPa $m^{1/2}$ were reported for ceramics fabricated by microwave sintering using Al_2O_3, Y_2O_3 and MgO as sintering additives [28].

IV. Conclusions

In this work, we have reported that a nearly fully dense β-Si_3N_4 ceramics with excellent mechanical properties was fabricated by spark plasma sintering (SPS). The following conclusions could be drawn:

- The fully dense β-Si_3N_4 ceramics with interlock microstructure with elongated grains was fabricated using α-Si_3N_4 powder and Al_2O_3 and yttria-stabilized zirconia (YSZ with 3 mol% Y_2O_3) as sintering additives.
- The Al_2O_3 and YSZ additive phases form the liquid glass phase at the grain boundary of Si_3N_4 at sintering temperature of 1600 °C by the reaction with the SiO_2 covering the Si_3N_4 particles in the starting powders.
- The β-Si_3N_4ceramics with interlock microstructure with elongated grains was obtained at 1600 °C by mechanism of dissolution-precipitation of the primary α-Si_3N_4 grains, showing excellent mechanical properties: Vickers hardness of 16.15 GPa and fracture toughness K_{IC} of 6.75 MPa $m^{1/2}$.

Acknowledgement: The work was supported by the National Natural Science Foundation of China (Nos: 51571144 and 11504239) and Shenzhen Science and Technology Research Grant (Nos. JCYJ 20150827155136104, JCYJ 20150324141711684).

References

1. M. Bengisu, *Engineering Ceramics*, Springer, Berlin 2001.
2. J.Q. Li, P. Xiao, "Joining ceramic to metal using a powder metallurgy method for high temperature applications", *J. Mater. Sci.*, **36** (2001) 1383–1387.
3. F.S. Liu, X.P. Chen, H.X. Xie, W.Q. Ao, J.Q. Li, "Negative thermal expansion of $Sc_{2-x}Ga_xW_3O_{12}$ solid solution", *Acta Phys. Sin.*, **59** (2010) 3350–3356.
4. J.Q. Li, P. Xiao, "Joining alumina using an alumina/metal composite", *J. Eur. Ceram. Soc.*, **22** (2002) 1225–1233.
5. J.Q. Li, P. Xiao, "Fabrication and characterisation of silicon carbide/superalloy interfaces", *J. Eur. Ceram. Soc.*, **24** (2004) 2149–2156.
6. F.L. Rile, "Silicon nitride and related materials", *J. Am. Ceram. Soc.*, **83** (2000) 245–265.
7. D.W. Freitag, "In situ processed Si_3N_4 whiskers in the system barium aluminosilicate-Si_3N_4", *Mater. Sci. Eng. A*, **195** (1995) 197–205.
8. H.O. Pierson, *Handbook of Refractory Carbides and Nitrides Properties, Characteristics, Processing and Applications*, Noyes Publications, Westwood, New Jersey, 1996.
9. J.L. Li, F. Chen, J.Y. Niu, Y. Yang, Z. Wang, "Dielectric properties of silicon nitride ceramics prepared by low temperature spark plasma sintering technique", *J. Ceram. Process. Res.*, **12** (2011) 236–239.
10. M. Suganuma, Y. Kitagawa, S. Wada, "Pulsed electric current sintering of silicon nitride", *J. Am. Ceram. Soc.*, **86** (2003) 387–394.
11. Z.J. Shen, Z. Zhao, H. Peng, M. Nygren, "Formation of tough interlocking microstructures in silicon nitride ceramics by dynamic ripening", *Nature*, **417** (2002) 266–269.
12. W.M. Guo, L.X. Wu, T. Ma, Y. You, H.T. Lin, "Rapid fabrication of Si_3N_4 ceramics by reaction-bonding and pressureless sintering", *J. Eur. Ceram. Soc.*, **36** (2016) 3919–3924.
13. A. Alem, M.D. Pugh, R. Drew, "Reaction bonded silicon nitride foams: the influence of iron disilicide on microstructure and mechanical strength", *Ceram. Int.*, **41** (2015) 4966–4974.
14. Y.J. Zhao, Y.J. Zhang, H.Y. Gong, H.B. Sun, Q.S. Li, "Gas pressure sintering of BN/Si_3N_4 wave transparent material with Y_2O_3-MgO nanopowders addition", *Ceram. Int.*, **40** (2014) 13537–13541.
15. W.M. Guo, L.X. Wu, T. Ma, S.X. Gu, Y. You, H.T. Lin, S.H. Wu, G.J. Zhang, "Chemical reactivity of hot-pressed Si_3N_4-ZrB_2 ceramics at 1500–1700 °C", *J. Eur. Ceram. Soc.*, **35** (2015) 2973–2979.
16. C. Hu, F. Li, D. Qu, Q. Wang, R. Xie, H. Zhang, S. Peng, Y. Bao, Y. Zhou, *Developments in Hot Pressing (HP) and Hot Isostatic Pressing (HIP) of Ceramic Matrix Composites, Advances in Ceramic Matrix Composites*, Woodhead Publishing, 2014.
17. M.Y. Zhou, J. Zhong, J. Zhao, D. Rodrigo, Y.B. Cheng, "Microstructures and properties of Si_3N_4/TiN composites sintered by hot pressing and spark plasma sintering", *Mater. Res. Bull.*, **48** (2013) 1927–1933.
18. X. Xu, T. Nishimura, N. Hirosaki, R.J. Xie, Y.C. Zhu, Y. Yamamoto, H. Tanaka, "New strategies for preparing nanosized silicon nitride ceramics", *J. Am. Ceram. Soc.*, **88** (2005) 934–937.
19. L. Bai, X.D. Mao, W.P. Shen, C.C. Ge, "Comparative study of beta-Si_3N_4 powders prepared by SHS sintered by spark plasma sintering and hot pressing", *J. Univ. Sci. Technol.*, **14** (2007) 271–275.
20. C.H. Lee, H.H. Lu, C.A. Wang, W.T. Lo, P.K. Nayak, J.L. Huang, "Microstructure and fracture behavior of beta-Si_3N_4 based nanoceramics", *Ceram. Int.*, **37** (2011) 641–645.
21. S. Bahrami, M. Zakeri, A. Faeghinia, M.R. Rahimipour, "Spark plasma sintering of silicon nitride/barium aluminum silicate composite", *Ceram. Int.*, **43** (2017) 9153–9157.
22. E. Ewais, M. Attia, A. Abousree-Hegazy, R.K. Bordia, "Investigation of the effect of ZrO_2 and ZrO_2/Al_2O_3 additions on the hot-pressing and properties of equimolecular mixtures of alpha- and beta-Si_3N_4", *Ceram. Int.*, **36** (2010) 1327–1338.
23. G.R. Anstis, P. Chantikul, B.R. Lawn, D.B. Marshall, "A critical evaluation of indentation techniques for measuring fracture toughness: I, Direct crack measurements", *J. Am. Ceram. Soc.*, **64** (1981) 533–538.
24. O.A. Lukianova, V.Y. Novikov, A.A. Parkhomenko, V.V.

Sirota, V.V. Krasilniko, "Microstructure of spark plasma-sintered silicon nitride ceramics", *Nanoscale Res. Lett.*, **12** (2017) 293.
25. M. Belmonte, J. Gonzalez-Julian, P. Miranzo, M. Osendi, "Spark plasma sintering: A powerful tool to develop new silicon nitride-based materials", *J. Eur. Ceram. Soc.*, **30** (2010) 2937–2946.
26. H. Hayashi, K. Hirao, M. Toriyama, S. Kanzaki, "$MgSiN_2$ addition as a means of increasing the thermal conductivity of beta-silicon nitride", *J. Am. Ceram. Soc.*, **84** (2001) 3060–3062.
27. J.S. Moya, J.F. Bartolome, P. Pena, "Quaternary equilibrium diagrams ZrO_2-Al_2O_3-SiO_2-(CaO, MgO, TiO_2). A powerful tool for the development of new materials by reaction sintering", *Bol. Soc. Esp. Ceram. V.*, **50** (2011) 291–300.
28. W.W. Xu, Z.B. Yin, J.T. Yuan, Z.H. Wang, Y.H. Fang, "Effects of sintering additives on mechanical properties and microstructure of Si_3N_4 ceramics by microwave sintering", *Mater. Sci. Eng. A*, **684** (2017) 127–134.